



Facile Synthesis of Manganese Cobalt Oxide/Nickel Cobalt Oxide Composites for High-Performance Supercapacitors

Wang Chen Huo^{1†}, Xiao Li Liu^{1†}, Yun Song Yuan^{2*}, Nan Li³, Tian Lan³, Xiao Ying Liu⁴ and Yu Xin Zhang^{1*}

OPEN ACCESS

Edited by:

Qiaobao Zhang,
Xiamen University, China

Reviewed by:

Shuge Dai,
Zhengzhou University, China
Jianglan Shui,
Beihang University, China
Kexin Yao,
King Abdullah University of Science
and Technology, Saudi Arabia
Shuangxi Xing,
Northeast Normal University, China
Limin Jin,
Shenzhen Graduate School of Harbin
Institute of Technology, China

*Correspondence:

Yun Song Yuan
yuan_ys@cqu.edu.cn
Yu Xin Zhang
zhangyuxin@cqu.edu.cn

[†]These authors have contributed
equally to this work

Specialty section:

This article was submitted to
Nanoscience,
a section of the journal
Frontiers in Chemistry

Received: 15 September 2018

Accepted: 19 December 2018

Published: 17 January 2019

Citation:

Huo WC, Liu XL, Yuan YS, Li N, Lan T,
Liu XY and Zhang YX (2019) Facile
Synthesis of Manganese Cobalt
Oxide/Nickel Cobalt Oxide
Composites for High-Performance
Supercapacitors. *Front. Chem.* 6:661.
doi: 10.3389/fchem.2018.00661

¹ State Key Laboratory of Mechanical Transmissions, College of Materials Science and Engineering, Chongqing University, Chongqing, China, ² College of Urban Construction and Environmental Engineering, Chongqing University, Chongqing, China, ³ Aerospace Institute of Advanced Materials & Processing Technology, Beijing, China, ⁴ Engineering Research Center for Waste Oil Recovery Technology and Equipment, Ministry of Education, College of Environment and Resources, Chongqing Technology and Business University, Chongqing, China

Transition metal oxides (TMOs) with spinel structures have a promising potential as the electrode materials for supercapacitors application owing to its outstanding theoretical capacity, good redox activity, and eco-friendly feature. In this work, MnCo₂O_{4.5}@NiCo₂O₄ nanowire composites for supercapacitors has been successfully fabricated by using a mild hydrothermal approach without any surfactant. The morphology and physicochemical properties of the prepared products can be well-controlled by adjusting experimental parameters of preparation. The double spinel composite exhibits a high specific capacitance of 325 F g⁻¹ (146 C g⁻¹) and 70.5% capacitance retention after 3,000 cycling tests at 1 A g⁻¹.

Keywords: transition metal oxides, spinel structure, composites, supercapacitor, MnCo₂O_{4.5}@NiCo₂O₄ nanowire

INTRODUCTION

The rising concerns about environmental crisis and increasing demand of renewable energy sources have attracted extensive attention for developing a secure, high-performance and sustainable storage technology (Lukatskaya et al., 2016; Zhang et al., 2018a). Recently, various energy storage technologies have emerged, such as lithium ion batteries (Zheng et al., 2018), Li-ion sulfur batteries (Sun et al., 2018) and supercapacitors (Qu et al., 2017) etc. Supercapacitors, also named as electrochemical capacitors (ECs), will be one of the most desirable power devices of next generation, owing to their high power density (Simon and Gogotsi, 2008), rapid charging-discharging rate (Miller and Simon, 2008), and excellent cycle stability (Dai et al., 2018). Various materials have been investigated as electrodes for ECs, such as carbon materials (Zhao et al., 2010; Niu et al., 2013; Zhang et al., 2018b), transition metal oxides (TMOs) (Liu et al., 2012; Nam et al., 2012) and conductive polymers (Lim et al., 2015). Generally, TMOs are superior in specific capacitance and stability. Their specific capacitance is 10~100 times of carbon materials, and they have better stability than conductive polymers. Among the TMOs, the spinel structures, especially spinel ternary TMOs, including the MnCo₂O_{4.5} (Li et al., 2014), NiCo₂O₄ (Wang C. et al., 2016), and ZnCo₂O₄ (Wu et al., 2015) etc., have been extensively investigated and exhibited an excellent electrochemical performance as electrode materials for ECs, due to its extremely high theoretical specific capacitance, good redox activity, and eco-friendliness (Qiu et al., 2018; Parveen et al., 2019), thus implying that these could be the most potential electrode materials for next-generation ECs.

Over the past few years, numerous researchers have been devoted to develop new strategies to enhance the electrochemical performance of NiCo₂O₄ nanomaterials for ECs electrodes (Sun et al., 2016). For example, Wang C. et al. (2016) reported that the NiCo₂O₄ nanoneedle was directly anchored on the Ni foam and carbon fabrics, respectively, via a facile hydrothermal method following with a calcination process in air. This strategy would enhance the combination of electrode material and substrate for improving the electrical conductivity and facilitating electrochemical performance. Sun et al. (2016) found that the porous NiCo₂O₄ nanograss supported on Ni foam shown a surprisingly high specific capacitance of 807.7 F g⁻¹ at 1 mA cm⁻² (0.38 A g⁻¹) after suffering the hydrogenation process for 3 h, which is ascribed to the formation of oxygen vacancies in disordered surface layers during the hydrogenation process and enhance the electrical conductivity. And there are many other strategies to improve the agglomeration of nanomaterials and facilitating contacting of electrolyte and electrode to promote the performance, such as NiCo₂O₄@3DNF framework (Parveen et al., 2019) and Co₉S₈@NiCo₂O₄ nanobrushes (Liu et al., 2019) etc. However, the price of Ni is eight times than the Mn (Information comes from the SMM Information & Technology Co, Ltd.), the high cost severely restricted its commercial applications. Hence, utilizing Mn to substitute Ni or constructing the Mn-Co-O@Ni-Co-O double spinel composites, should be a feasible and effective method for reducing the cost and promoting its application. Unfortunately, the Mn substituted spinel structure always exhibited the poor specific capacitance (Li et al., 2014, 2015; Hao et al., 2015; Wang K. et al., 2016). Thus, fabricating the Mn-Co-O@Ni-Co-O double spinel composites would be an alternative preferable strategy, which is not only decreasing the commercial applications cost, but also improving the electrochemical performance of double spinel composites for ECs via utilizing the synergistic effect of the core and shell.

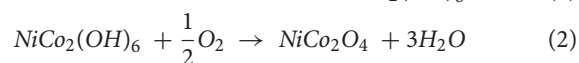
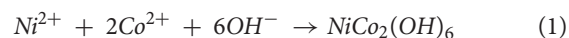
Herein, the core-shell MnCo₂O_{4.5}@NiCo₂O₄ double spinel structures were successfully synthesized by a facile hydrothermal route without any surfactant, where the core, hierarchical MnCo₂O_{4.5} nanowires with a diameter of 300~500 nm was provided by Li et al. (2015). The prepared MnCo₂O_{4.5}@NiCo₂O₄ hybrids exhibit a promising electrochemical performance via comparing with literature results of selected samples which have similar components and structures (Table 1) (Wu et al., 2011; Kuang et al., 2014; Li et al., 2014, 2015; Hao et al., 2015; Sun et al., 2016; Wang C. et al., 2016; Wang K. et al., 2016). This strategy not only diminishes the dosage of Ni, but also elevates the electrochemical performance of the double spinel composites for ECs, which are favor of the commercial applications for next generation energy storage devices.

EXPERIMENTAL SECTION

Materials Synthesis

MnCo₂O_{4.5} nanowires provided by Li's group were adopted as the reaction substrates in the experimental. The synthesis procedure of MnCo₂O_{4.5} has been reported in detail in Li's work (Li et al., 2015). Figure 1 shows the schematic illustration of the MnCo₂O_{4.5}@NiCo₂O₄ nanowires, and the composites

were fabricated as follows: 0.001 mol Ni(NO₃)₂·6H₂O, 0.002 mol Co(NO₃)₂·6H₂O, 0.002 mol NH₄F and 0.005 mol urea were dissolved in 35 mL deionized water at room temperature, then 20 mg MnCo₂O_{4.5} were added into the mixture, supplemented by ultrasonic treatment until the MnCo₂O_{4.5} powder were dispersed uniformly. Then the suspension was put in the Teflon-lined stainless autoclave, sealed and heated at 120°C for 6 and 12 h, respectively. After cooling down to room temperature, collected precipitates were washed several times using ethanol and deionized water to remove the attached reaction products and/or residual reactants, then put into the vacuum oven at 60°C to dry. Finally, the metal hydroxides were calcined at 350°C for 2 h to convert into metal oxides most likely as described by the following equations (Xu and Wang, 2011):



Characterization

X-ray photoelectron spectroscopy (Kratos XSAM800, XPS), the powder X-ray diffraction (D/max 2500, Cu K α , XRD) and thermogravimetric analyzer-differential scanning calorimeter (NETZSCH STA 449C, TGA-DSC) were used to characterize the crystallinity and components of prepared materials. Morphological structure was analyzed by scanning electron microscopy (Zeiss Auriga FIB/SEM). The detailed structures of the materials were collected by transmission electron microscopy (FEI TECNAI G2 F20, TEM).

Electrochemical Measurement

In this work, the three-electrode configuration with the potentiostat/galvanostat model (CHI660E electrochemical workstation) was employed to detect the electrochemical performance of the prepared electrode materials, where nickel foam (1 × 1 cm) supported MnCo₂O_{4.5}@NiCo₂O₄ composites worked as the working electrode, saturated calomel electrode (SEC) served as the reference electrode and platinum plate acted as the counter electrode in 3 M KOH electrolyte. The materials for the preparation of working electrode are active materials, acetylene black and polyvinylidene difluoride (PVDF) (mass ratio, 7:2:1). After calculation, the net mass of MnCo₂O_{4.5}@NiCo₂O₄ loaded on each working electrode is 1.5 mg.

The cyclic voltammetry (CV) and charge-discharge (GCD) measurements were tested on a CHI660E electrochemical workstation. The CV curves were carried out at disparate scan rates between 0 and 0.5 V (vs. SCE), while the charge-discharge curves (0~0.45 V vs. SCE) were monitored at different current densities. The electrochemical impedance spectroscopy (EIS) plots were obtained over the frequency from 10⁻² to 10⁵ Hz with the 5 mV amplitude. The normalized specific capacitance (C, F g⁻¹) and (Q, C g⁻¹) was calculated from charge-discharge curves and following the equation (Dai et al., 2017):

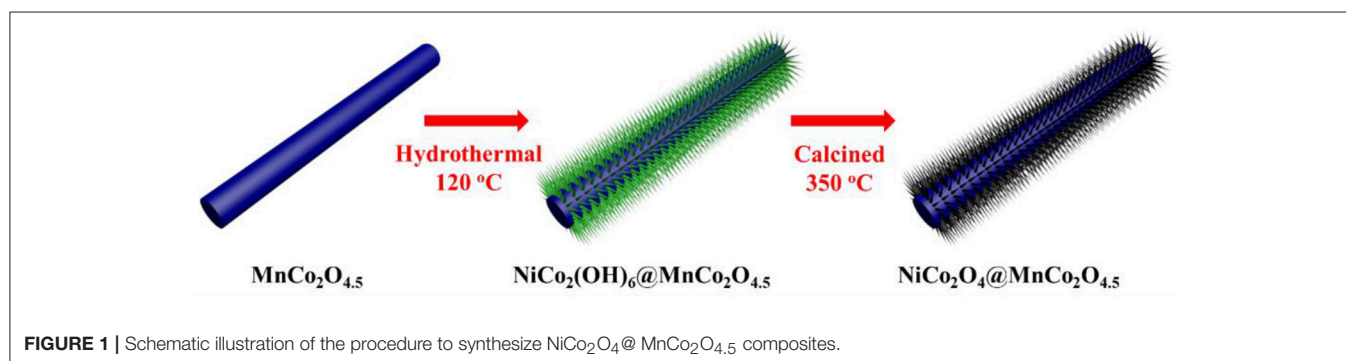
$$C = I\Delta t/\Delta Vm \quad (3)$$

$$Q = I\Delta t/m \quad (4)$$

TABLE 1 | Comparison of specific capacitances of selected literature results obtained from materials with similar components and this work.

Samples	Electrolyte	Test condition	Cs (F g ⁻¹)	References
MnCo ₂ O _{4.5}	1 M Na ₂ SO ₄	0.5 A g ⁻¹	80.2 F g ⁻¹	Li et al., 2015
MnCo ₂ O _{4.5}	1 M KOH	1 A g ⁻¹	118.8 F g ⁻¹	Li et al., 2014
MnCo ₂ O _{4.5}	1 M Na ₂ SO ₄	2 A g ⁻¹	114 F g ⁻¹	Wang C. et al., 2016
Carbon aerogel@MnCo ₂ O _{4.5}	1 M Na ₂ SO ₄	0.2 A g ⁻¹	269.9 F g ⁻¹	Hao et al., 2015
NiCo ₂ O ₄ @Ni foam	6 M KOH	1 mA cm ⁻²	807.7 F g ⁻¹	Sun et al., 2016
NiCo ₂ O ₄ @Ni foam	2 M KOH	1 A g ⁻¹	655 F g ⁻¹	Wang K. et al., 2016
NiCo ₂ O ₄	2 M KOH	1 A g ⁻¹	372 F g ⁻¹	Kuang et al., 2014
NiCo ₂ O ₄	1 M KOH	1 mA cm ⁻²	217 F g ⁻¹	Wu et al., 2011
MnCo ₂ O _{4.5} @NiCo ₂ O ₄	3 M KOH	1 A g ⁻¹	325 F g ⁻¹	This work

All values are derived from characterizations in three-electrode systems.



where I is the operated current (A), Δt the discharge time (s), m the mass of active electrode materials (g), and ΔV the potential window of discharge (V).

RESULTS AND DISCUSSION

The X-ray diffraction peaks of the prepared products were well-indexed to the cubic phase of MnCo₂O_{4.5} (JCPDS 32-0297) (**Figure 2A**) (Hao et al., 2015). No additional peak for other phase of MnCo₂O_{4.5} was observed and the sharp and narrow diffraction peaks forecast that the MnCo₂O_{4.5} microstructures have high crystallinity. The diffraction peaks of the MnCo₂O_{4.5}@NiCo₂O₄ have minor left shift (0.1°) compared with MnCo₂O_{4.5} (**Figure 2B**), which is ascribed the crystallinity of NiCo₂O₄ (JCPDS 20-0781) is very similar to MnCo₂O_{4.5} (Sun et al., 2016; Wang C. et al., 2016), but the lattice constant is tiny bigger than MnCo₂O_{4.5}. NiCo₂O₄ and MnCo₂O_{4.5} are both spinel structured crystals and have a high degree of lattice matching (~0.3% mis-match). The lattice parameters of MnCo₂O_{4.5} are 8.08*8.08*8.08<90.0*90.0*90.0>, and NiCo₂O₄ 8.11*8.11*8.11<90.0*90.0*90.0> and the **Figures 3A,B** show the crystal structure of MnCo₂O_{4.5} and NiCo₂O₄, respectively. Moreover, in the XRD results the peak intensities of the (311) and (440) planes are higher than others, therefore NiCo₂O₄ is most likely to grow along the (311) and (440) planes and completely coherent with MnCo₂O_{4.5} at the (311) and

(440) planes. **Figures 3C,D** shows the possible epitaxial growth patterns of MnCo₂O_{4.5}@NiCo₂O₄ as mentioned above.

Thermogravimetric (TGA) and differential scanning calorimetry (DSC) were performed at a 10°C min⁻¹ heating rate to investigate the thermal properties (**Figure 2C**). The TGA-DSC curve of the Ni-Co hydroxide on MnCo₂O_{4.5} is shown in **Figure 2C**. The evaporation of the physically adsorbed water resulted in the weight loss (about 3%) till 280°C. And the followed 17% weight loss between 280 and 400°C is most likely to be caused by the crystalliferous water loss and the decomposition of Ni-Co hydroxide. There is no obvious weight loss after 400°C. Based on these findings, 350°C is chosen and believed to be sufficient for calcination treatment of hydroxides.

SEM was adopted to investigate the morphologies of as-prepared composites. As shown in **Figure S1**, the MnCo₂O_{4.5} nanowires exhibit fibrous morphologies with smooth surface. The length MnCo₂O_{4.5} nanowires are several micrometers and the average diameter is about 300~500 nm. **Figures 4A,B** shows that NiCo₂O₄ nanowires with smaller diameter are successfully and uniformly grown on the surface of MnCo₂O_{4.5} nanowires. When the reaction time increases from 6 to 12 h, dense NiCo₂O₄ nanowires are observed (**Figure 4B**) with more nanowires locating within the unit area of MnCo₂O_{4.5} surface. The two insets in **Figures 4A,B** are the images of corresponding samples at higher magnifications. The EDS mapping demonstrates the uniform distribution of Mn, Ni,

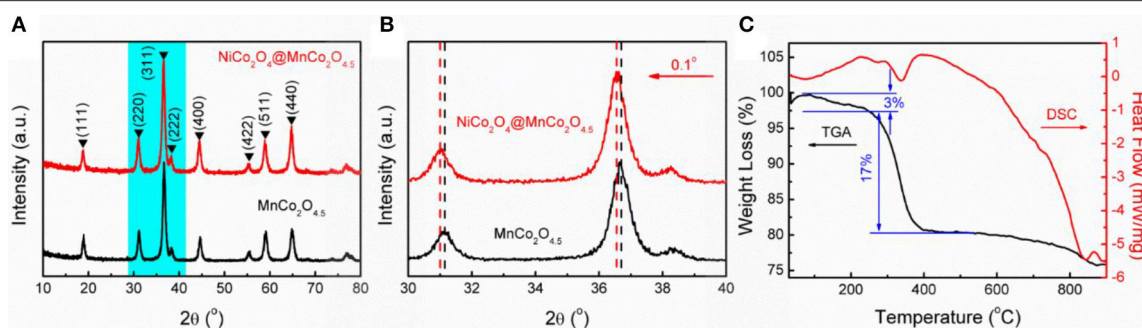


FIGURE 2 | (A) XRD patterns of MnCo₂O_{4.5} nanowires and MnCo₂O_{4.5}@NiCo₂O₄ composites. (B) The enlarged XRD patterns at the 2θ of 30–40. (C) TGA-DSC curves of Ni-Co hydroxide@MnCo₂O_{4.5} composites.

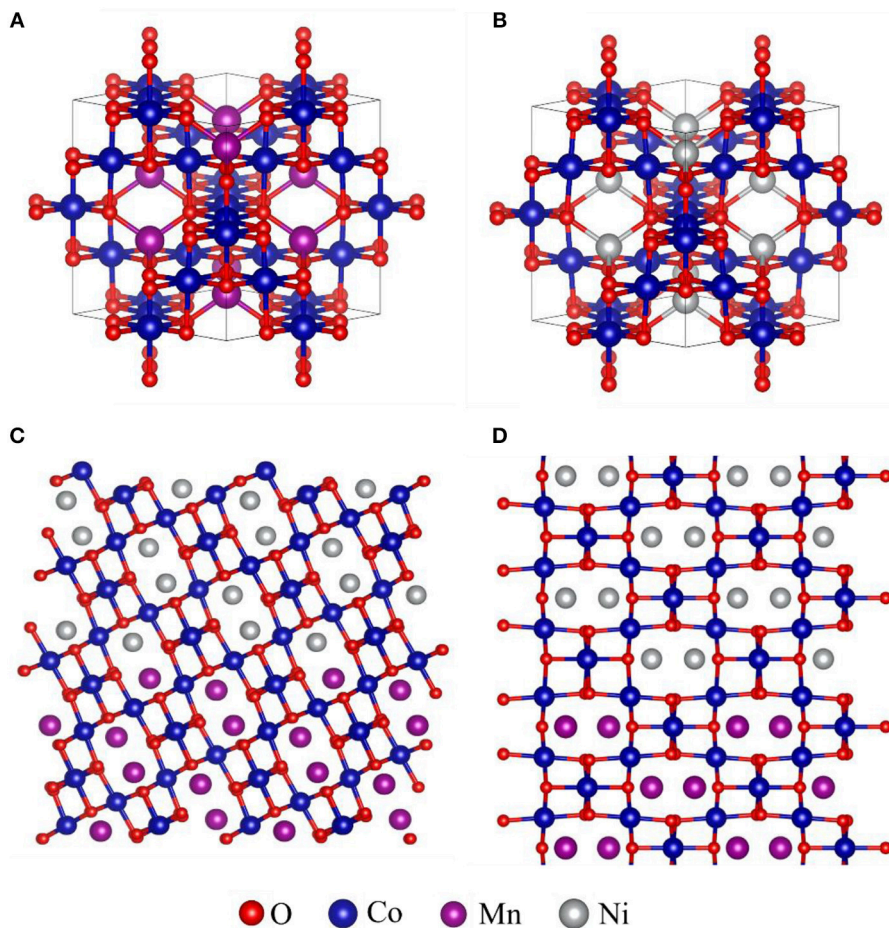
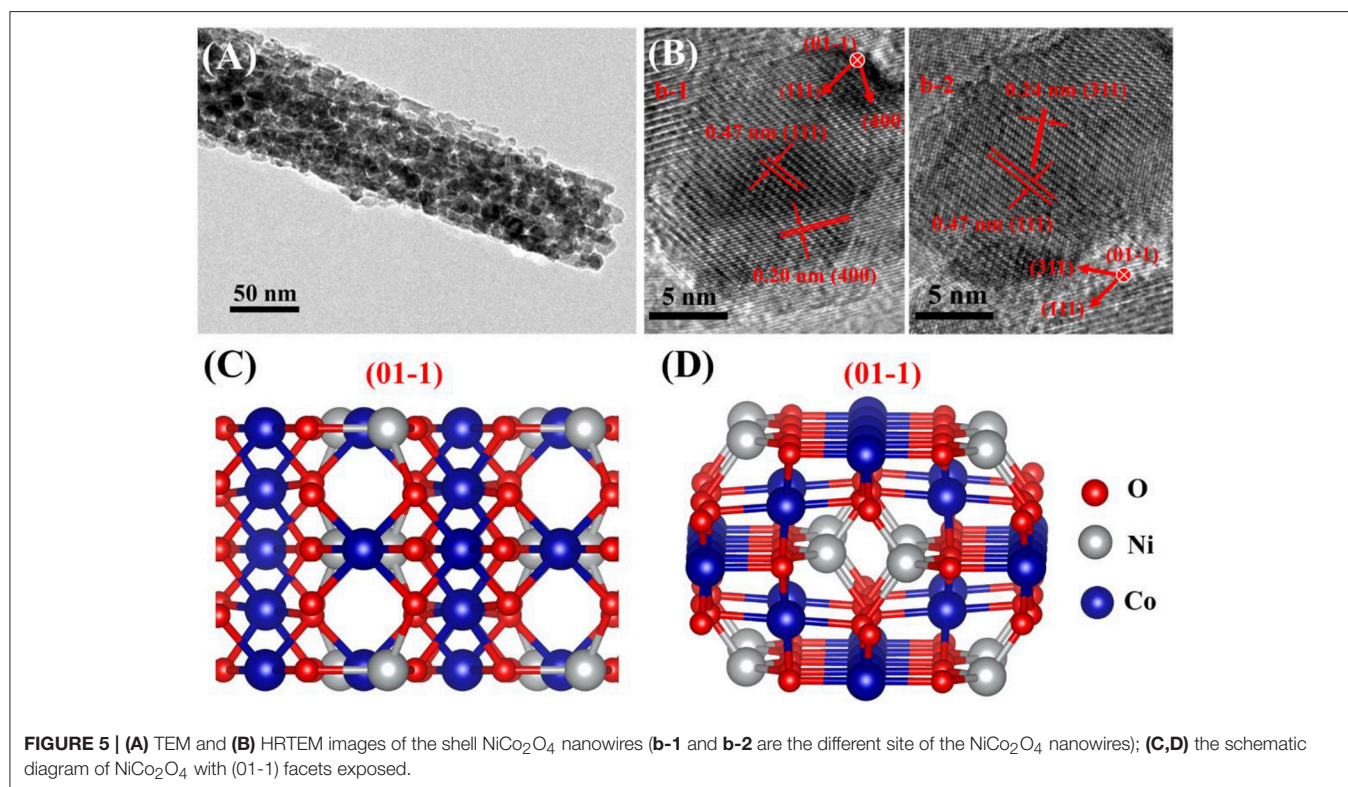
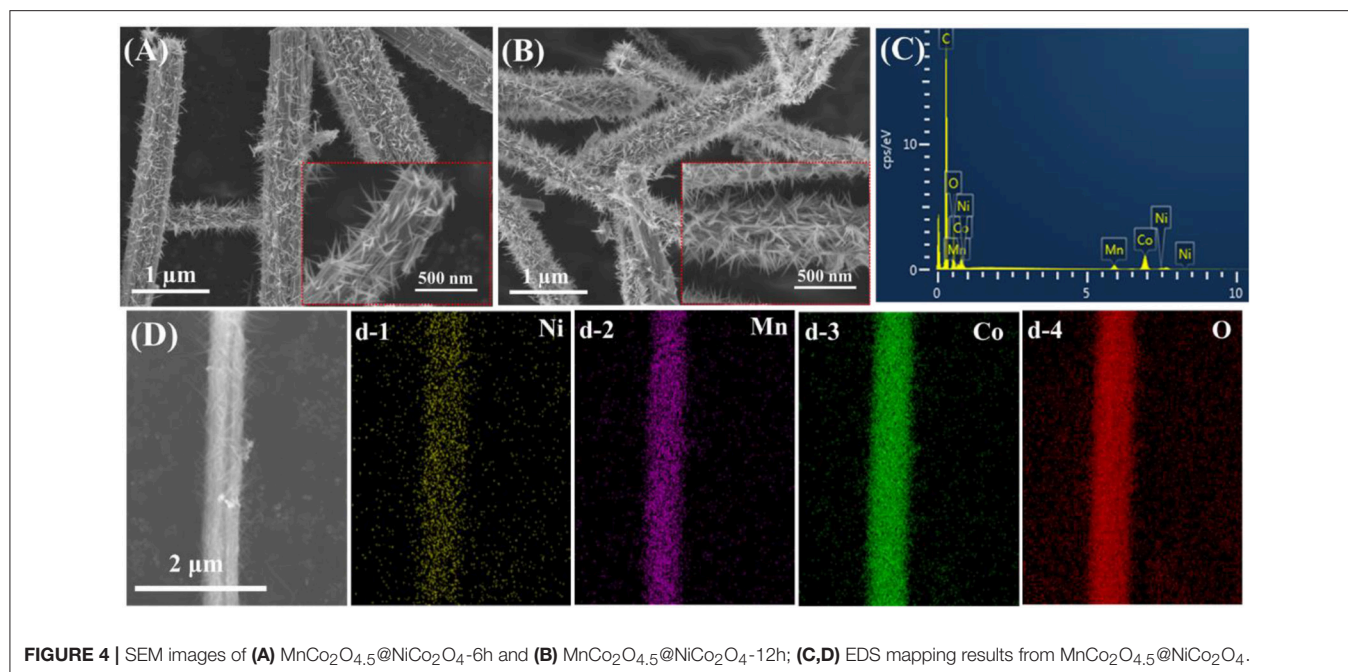


FIGURE 3 | The schematic diagram of MnCo₂O_{4.5} (A) and NiCo₂O₄ (B) crystal structure. Structure description for possible epitaxial growth patterns of MnCo₂O_{4.5}@NiCo₂O₄ (C) NiCo₂O₄ growing along (311) plane of MnCo₂O_{4.5}; (D) NiCo₂O₄ growing along (440) plane of MnCo₂O_{4.5}.

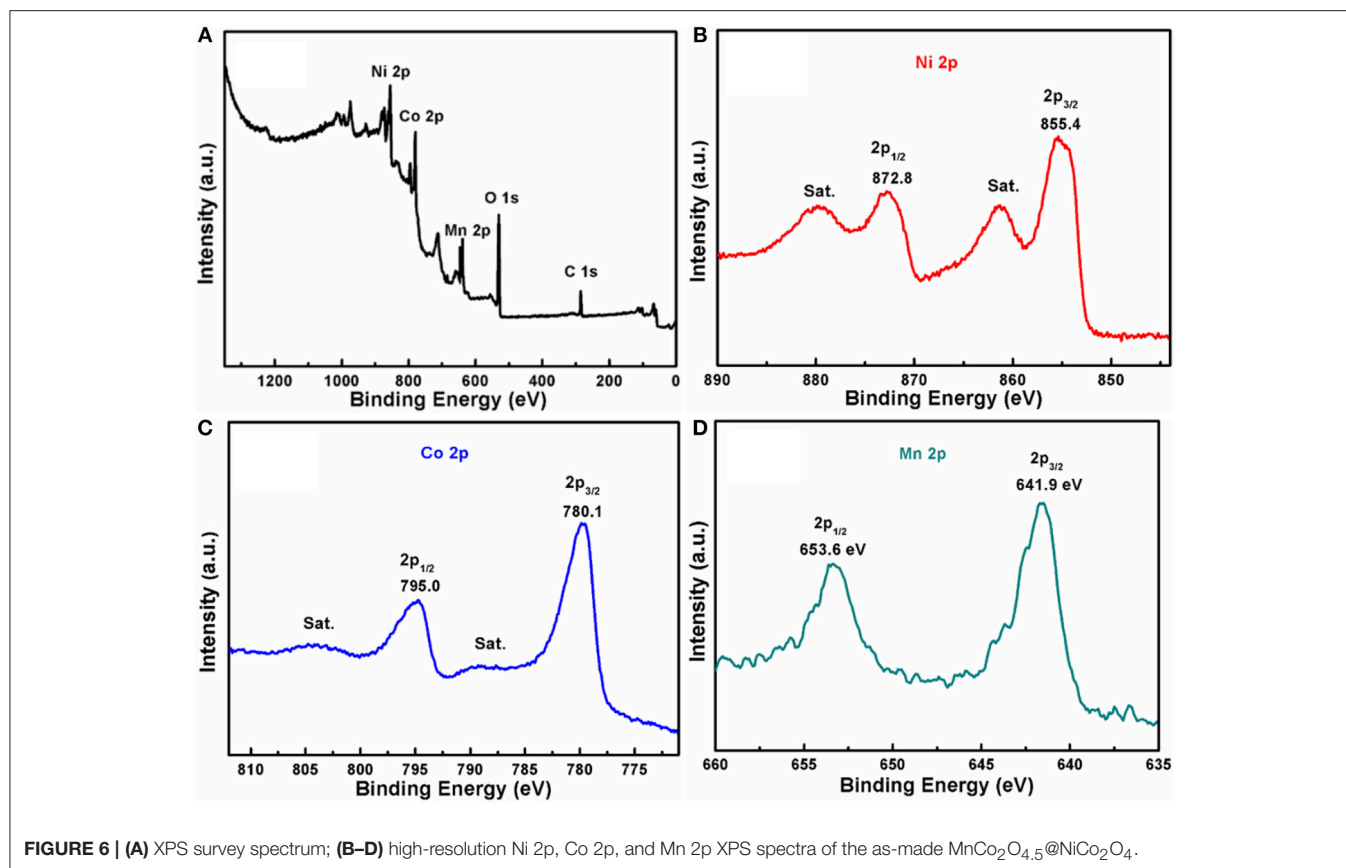
Co, and O (Figures 4C,D), suggesting successful fabrication of well-distributed MnCo₂O_{4.5}@NiCo₂O₄ nanowires and forming the core-shell structure. Furthermore, the detailed structural information of the coated NiCo₂O_{4.5} shell nanowires was collected by TEM at different magnifications (Figures 5A,B).

The primary NiCo₂O₄ nanowires have a diameter of 50~80 nm. High-resolution TEM (HRTEM, Figure 5B) image of the NiCo₂O₄ nanowires reveal well-resolved lattice fringe having an inter-planar spacing of 0.20 and 0.47 nm (b-1), which are well-consistent with the distance of the (400) and (111) plane of



NiCo₂O₄, respectively. And the (**b-2**) shows inter-planar spacing of 0.24 and 0.47 nm, which represent the (311) and (111) facet of NiCo₂O₄. Therefore, these results about the crystal structure and facets illustrate that the (01-1) facets of NiCo₂O₄ are exposed (Figures 5C,D).

XPS measurement was employed to reveal the composition and surface chemical states of the MnCo₂O_{4.5}@NiCo₂O₄, and the detailed results are shown in Figure 6. It can be clearly seen from survey spectrum (Figure 6A) that the MnCo₂O_{4.5}@NiCo₂O₄ consists of O, Ni, Co, and Mn elements, being consistent with



EDS results (Figure 3D). The high resolution XPS spectrum of Ni 2p (Figure 6B) reveals that two obvious shakeup satellites (indicated as “Sat.”) are close to two spin orbit doublets at 855.4 and 872.8 eV, which represents the Ni 2p_{3/2} and Ni 2p_{1/2} splitting in Ni²⁺ chemical state, respectively (Hareesh et al., 2016; Sun et al., 2016; Wang et al., 2017; Zhang et al., 2018b). In the Co 2p XPS spectrum, the spin orbit splitting to the Co 2p_{1/2} (795.0 eV) and Co 2p_{3/2} (780.1 eV) reaches 14.9 eV (Figure 6C), indicating the co-existence of Co²⁺ and Co³⁺ in MnCo₂O_{4.5}@NiCo₂O₄ (Wu et al., 2015; Liu et al., 2017; Wang et al., 2017). Likewise, the peaks of Mn element locating at 641.9 eV and 653.6 eV in Figure 6D consistent with Mn 2p_{3/2} and Mn 2p_{1/2}, respectively (Hui et al., 2016; Liu et al., 2017; Zhao et al., 2018; Zhu et al., 2018).

The electrochemical performance of the samples was analyzed by CV and GCD measurements. Figures 7A,B illustrates the CV and GCD curves of the three different electrodes at the same scan rate (100 mV S⁻¹) and current density (1 A g⁻¹), respectively. MnCo₂O_{4.5}@NiCo₂O_{4-12h} displays better rate performance with lower distortion compared with MnCo₂O_{4.5}@NiCo₂O_{4-6h} (Figure 7B). This is possibly due to the mass increasing of NiCo₂O₄ and the lower mass transport resistance within smaller interstitial regimes between the electrolyte and electrode materials. In Figure 7C, the CV curves of MnCo₂O_{4.5}@NiCo₂O_{4-12h} exhibit a quasi-reversible oxidative and reductive shape, indicating an ideal

capacitance characteristic and a good reversibility of the architectures with good electronic conductivity and low internal resistance (Zhu et al., 2015; Hui et al., 2016; Sun et al., 2016; Wang et al., 2017). With the increment of scan rates, slight distortion of curves is observed, implying the favorable rate ability. The galvanostatic charge-discharge results of MnCo₂O_{4.5}@NiCo₂O_{4-12h} are presented in Figure 7D. Similarly, pseudo-capacitive behaviors are observed and the shape of GCD curves is not triangular ones which are believed to be pure electrical double layer capacitors (EDLCs).

The symmetrical shapes of the charge side and discharge side indicate the good reversibility of the synthesized composites. The MnCo₂O_{4.5}@NiCo₂O_{4-12h} composites (Figure 7D) have a higher specific capacitance of 325 F g⁻¹ (146 C g⁻¹) than that of MnCo₂O_{4.5}@NiCo₂O_{4-6h} [162.5 F g⁻¹ (73 C g⁻¹), Figure 7B] at the same discharge current density (1 A g⁻¹), which is owing to its higher mass ratio of active NiCo₂O₄. Compared with pristine MnCo₂O_{4.5}, the electrochemical performance of synthesized core-shell composites is greatly improved based on the following two effects: MnCo₂O_{4.5}@NiCo₂O_{4-12h} has larger accessible surface area from loose NiCo₂O₄ shell layer which is built with isolated free-standing nanowires with smaller diameters; and shorter ion diffusion distance from smaller free-standing NiCo₂O₄ nanowires and interstitial regime between nanowires as well.

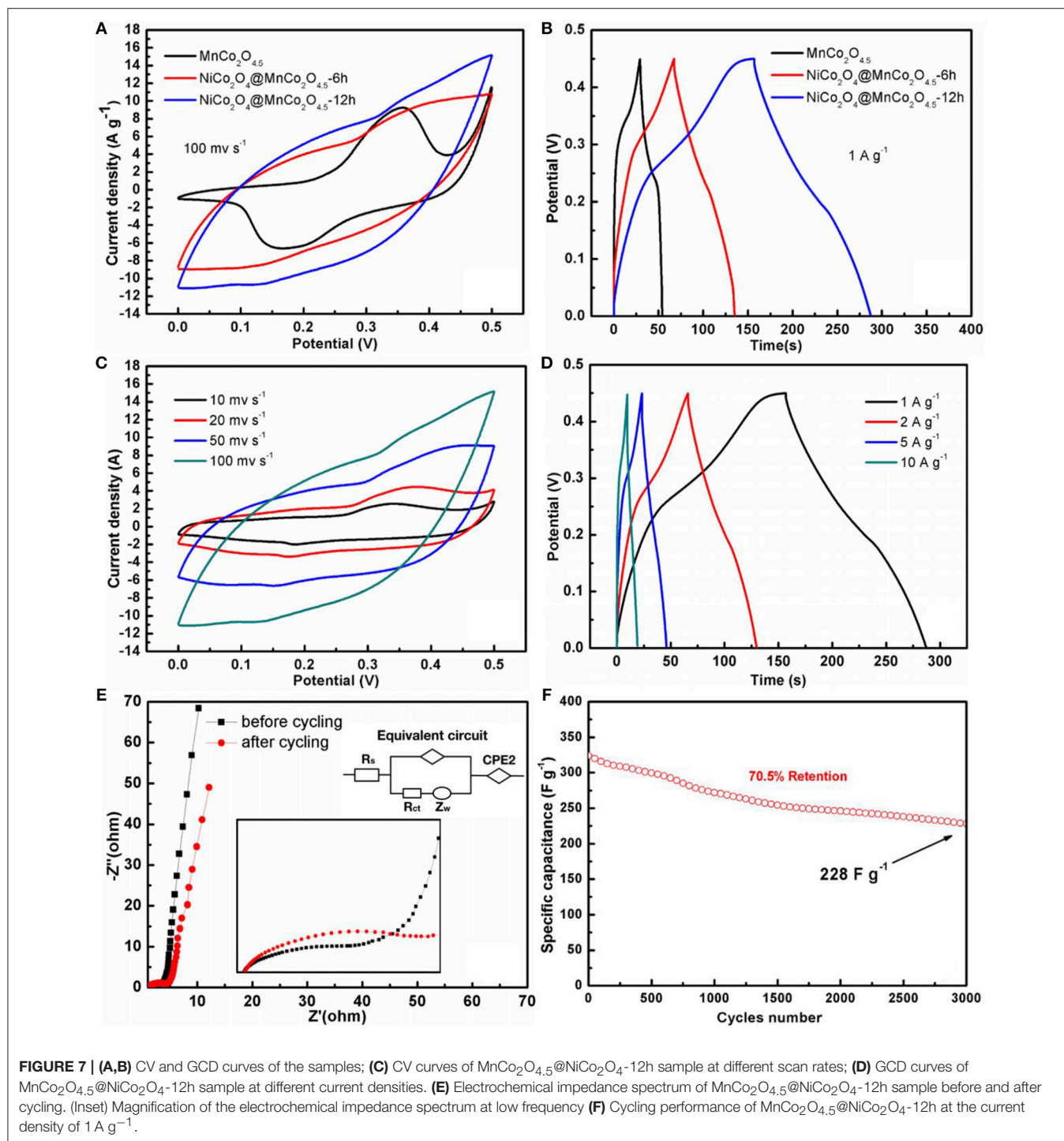


Figure 7E depicts the electrical impedance spectroscopy (EIS) of the composites before and after 3,000 cycling tests. The inset is magnified spectrum at low impedance region. The impedance spectrum is a semicircle parts at the high frequency and a linear curve at the low frequency. The intercept of the curves on the real axis reveals the total value of the ohmic resistance of electrolyte added with the resistance of the active

materials. After cycling test, the radius of the semicircle increased obviously while first intercept and slope of the linear part change slightly. The apparent increasing of semicircle radius means more difficult for charge transfer of active species inside the electrode materials. The minor increasing of first intercept and decreasing of slope indicate higher contacting impedance and mass transport resistance after cycling tests. All the changes

are derived from the potential structural damage of electrode materials during cycling tests. However, the overall capacitance retention is still up to 70.5% after 3,000 cycling tests (Figure 7F), which means this damage over cycling is at low level. This good cycling ability of MnCo₂O_{4.5}@NiCo₂O₄ is attributed to its unique one-dimensional structure. The one-dimensional structure has much free spaces between the nanowires, being able to accommodate the volume change of the materials during cycling and maintain the activity of the materials at high level.

CONCLUSIONS

The MnCo₂O_{4.5}@NiCo₂O₄ composites with core-shell structure has been successfully synthesized with a facile and green hydrothermal method for high performance supercapacitors. The nanostructures, morphology and electrochemical performance of the composites are fully demonstrated. The MnCo₂O_{4.5}@NiCo₂O₄ composites exhibit remarkable capacitive performance with maximum capacitances of 325 F g⁻¹ (146 C g⁻¹) and retention 70.5% of the initial capacitance after 3,000 cycles at 1 A g⁻¹. This excellent electrochemical performance of MnCo₂O_{4.5}@NiCo₂O₄ composites are attributed to the unique core-shell double spinel structures with shell built of isolated free-standing nanowires. The free spaces between nanowires are able to provide channels for mass transfer of active species and accommodate the volume change during cycling.

REFERENCES

- Dai, S., Liu, Z., Zhao, B., Zeng, J., Hu, H., Zhang, Q., et al. (2018). A high-performance supercapacitor electrode based on N-doped porous graphene. *J. Power Sources* 387, 43–48. doi: 10.1016/j.jpowsour.2018.03.055
- Dai, S., Zhao, B., Qu, C., Chen, D., Dang, D., Song, B., et al. (2017). Controlled synthesis of three-phase Ni₃S₂/rGO nanoflake electrodes for hybrid supercapacitors with high energy and power density. *Nano Energy* 33, 522–531. doi: 10.1016/j.nanoen.2017.01.056
- Hao, P., Zhao, Z., Li, L., Tuan, C.-C., Li, H., Sang, Y., et al. (2015). The hybrid nanostructure of MnCo₂O_{4.5} nanoneedle/carbon aerogel for symmetric supercapacitors with high energy density. *Nanoscale* 7, 14401–14412. doi: 10.1039/c5nr04421a
- Hareesh, K., Shateesh, B., Joshi, R. P., Dahiwal, S. S., Bhoraskar, V. N., Haram, S. K., et al. (2016). PEDOT: PSS wrapped NiFe₂O₄/rGO tertiary nanocomposite for the super-capacitor applications. *Electrochim. Acta* 201, 106–116. doi: 10.1016/j.electacta.2016.03.205
- Hui, K. N., Hui, K. S., Tang, Z., Jadhav, V. V., and Xia, Q. X. (2016). Hierarchical chestnut-like MnCo₂O₄ nanoneedles grown on nickel foam as binder-free electrode for high energy density asymmetric supercapacitors. *J. Power Sources* 330, 195–203. doi: 10.1016/j.jpowsour.2016.08.116
- Kuang, M., Zhang, W., Guo, X. L., Yu, L., and Zhang, Y. X. (2014). Template-free and large-scale synthesis of hierarchical dandelion-like NiCo₂O₄ microspheres for high-performance supercapacitors. *Ceram. Int.* 40, 10005–10011. doi: 10.1016/j.ceramint.2014.02.099
- Li, F., Li, G., Chen, H., Jia, J. Q., Dong, F., Hu, Y. B., et al. (2015). Morphology and crystallinity-controlled synthesis of manganese cobalt oxide/manganese dioxides hierarchical nanostructures for high-performance supercapacitors. *J. Power Sources* 296, 86–91. doi: 10.1016/j.jpowsour.2015.07.029
- Li, W., Xu, K., Song, G., Zhou, X., Zou, R., Yang, J., et al. (2014). Facile synthesis of porous MnCo₂O_{4.5} hierarchical architectures for high-

AUTHOR CONTRIBUTIONS

YXZ and YSY designed the research. WCH, XLL, and XYL performed the experiments. NL and TL carried out the partial experimental characterization. All authors incorporated in the discussion of experimental results.

ACKNOWLEDGMENTS

We gratefully thank the financial support of the Fundamental Research Funds for the Central Universities (2018CDYJSY0055 and 106112017CDJXSYY0001), the National Natural Science Foundation of China (Grant no. 21576034), the key scientific and technological projects of Chongqing Municipal Education Commission (KJZD-K201800801), Joint Funds of the National Natural Science Foundation of China-Guangdong (Grant no. U1801254), the project funded by Chongqing Special Postdoctoral Science Foundation (XmT2018043), and Technological projects of Chongqing Municipal Education Commission (KJZDK201800801). We also thank the Electron Microscopy Center of Chongqing University for materials characterizations.

SUPPLEMENTARY MATERIAL

The Supplementary Material for this article can be found online at: <https://www.frontiersin.org/articles/10.3389/fchem.2018.00661/full#supplementary-material>

- rate supercapacitors. *CrystEngComm* 16, 2335–2339. doi: 10.1039/c3ce42581a
- Lim, Y.-G., Park, M.-S., Kim, K. J., Jung, K.-S., Kim, J. H., Shahabuddin, M., et al. (2015). Incorporation of conductive polymer into soft carbon electrodes for lithium ion capacitors. *J. Power Sources* 299, 49–56. doi: 10.1016/j.jpowsour.2015.08.083
- Liu, J.-L., Fan, L.-Z., and Qu, X. (2012). Low temperature hydrothermal synthesis of nano-sized manganese oxide for supercapacitors. *Electrochim. Acta* 66, 302–305. doi: 10.1016/j.electacta.2012.01.095
- Liu, Q., Hong, X. D., Zhang, X., Wang, W., Guo, W. X., Liu, X. Y., et al. (2019). Hierarchically structured Co₉S₈@NiCo₂O₄ nanobrushes for high-performance flexible asymmetric supercapacitors. *Chem. Eng. J.* 356, 985–993. doi: 10.1016/j.cej.2018.09.095
- Liu, S., Lee, S. C., Patil, U., Shackery, I., Kang, S., Zhang, K., et al. (2017). Hierarchical MnCo-layered double hydroxides@Ni(OH)₂ core-shell heterostructures as advanced electrodes for supercapacitors. *J. Mater. Chem. A* 5, 1043–1049. doi: 10.1039/c6ta07842g
- Lukatskaya, M. R., Dunn, B., and Gogotsi, Y. (2016). Multidimensional materials and device architectures for future hybrid energy storage. *Nat. Commun.* 7:12647. doi: 10.1038/ncomms12647
- Miller, J. R., and Simon, P. (2008). Materials science–Electrochemical capacitors for energy management. *Science* 321, 651–652. doi: 10.1126/science.1158736
- Nam, I., Kim, G.-P., Park, S., Park, J., Kim, N. D., and Yi, J. (2012). Fabrication and design equation of film-type large-scale interdigitated supercapacitor chips. *Nanoscale* 4, 7350–7353. doi: 10.1039/c2nr31961f
- Niu, Z., Zhang, L., Liu, L., Zhu, B., Dong, H., and Chen, X. (2013). All-solid-state flexible ultrathin micro-supercapacitors based on graphene. *Adv. Mater.* 25, 4035–4042. doi: 10.1002/adma.201301332
- Parveen, N., Al-Jaafari, A. I., and Han, J. I. (2019). Robust cyclic stability and high-rate asymmetric supercapacitor based on orange peel-derived nitrogen-doped porous carbon and intercrossed interlinked urchin-like NiCo₂O₄@3DNF

- framework. *Electrochim. Acta* 293, 84–96. doi: 10.1016/j.electacta.2018.08.157
- Qiu, W. D., Xiao, H. B., Yu, M. H., Li, Y., and Lu, X. H. (2018). Surface modulation of NiCo₂O₄ nanowire arrays with significantly enhanced reactivity for ultrahigh-energy supercapacitors. *Chem. Eng. J.* 352, 996–1003. doi: 10.1016/j.cej.2018.04.118
- Qu, C., Zhao, B., Jiao, Y., Chen, D., Dai, S., Deglee, B. M., et al. (2017). Functionalized bimetallic hydroxides derived from metal–organic frameworks for high-performance hybrid supercapacitor with exceptional cycling stability. *ACS Energy Lett.* 2, 1263–1269. doi: 10.1021/acseenergylett.7b00265
- Simon, P., and Gogotsi, Y. (2008). Materials for electrochemical capacitors. *Nat. Mater.* 7, 845–854. doi: 10.1038/nmat2297
- Sun, D. S., Li, Y. H., Wang, Z. Y., Cheng, X. P., Jaffer, S., and Zhang, Y. F. (2016). Understanding the mechanism of hydrogenated NiCo₂O₄ nanogras supported on Ni foam for enhanced-performance supercapacitors. *J. Mater. Chem. A* 4, 5198–5204. doi: 10.1039/c6ta00928j
- Sun, J., Zeng, Q., Lv, R., Lv, W., Yang, Q.-H., Amal, R., et al. (2018). A Li-ion sulfur full cell with ambient resistant Al-Li alloy anode. *Energy Storage Mater.* 15, 209–217. doi: 10.1016/j.ensm.2018.04.003
- Wang, C., Zhou, E., Deng, X., Shao, M., Huang, J., Wei, X., et al. (2016). Three-dimensionally porous NiCo₂O₄ nanoneedle arrays for high performance supercapacitor. *Sci. Adv. Mater.* 8, 1298–1304. doi: 10.1166/sam.2016.2725
- Wang, K., Xu, J., Lu, A., Shi, Y., and Lin, Z. (2016). Coordination polymer template synthesis of hierarchical MnCo₂O_{4.5} and MnNi₆O₈ nanoparticles for electrochemical capacitors electrode. *Solid State Sci.* 58, 70–79. doi: 10.1016/j.solidstatesciences.2016.06.001
- Wang, T., Zhang, S., Yan, X., Lyu, M., Wang, L., Bell, J., et al. (2017). 2-methylimidazole-derived Ni-Co layered double hydroxide nanosheets as high rate capability and high energy density storage material in hybrid supercapacitors. *ACS Appl. Mater. Interfaces* 9, 15510–15524. doi: 10.1021/acsnano.7b02987
- Wu, C., Cai, J., Zhang, Q., Zhou, X., Zhu, Y., Li, L., et al. (2015). Direct growth of urchin-like ZnCo₂O₄ microspheres assembled from nanowires on nickel foam as high-performance electrodes for supercapacitors. *Electrochim. Acta* 169, 202–209. doi: 10.1016/j.electacta.2015.04.079
- Wu, Y. Q., Chen, X. Y., Ji, P. T., and Zhou, Q. Q. (2011). Sol-gel approach for controllable synthesis and electrochemical properties of NiCo₂O₄ crystals as electrode materials for application in supercapacitors. *Electrochim. Acta* 56, 7517–7522. doi: 10.1016/j.electacta.2011.06.101
- Xu, S., and Wang, Z. L. (2011). One-dimensional ZnO nanostructures: solution growth and functional properties. *Nano Res.* 4, 1013–1098. doi: 10.1007/s12274-011-0160-7
- Zhang, Q., Chen, H., Luo, L., Zhao, B., Luo, H., Han, X., et al. (2018a). Harnessing the concurrent reaction dynamics in active Si and Ge to achieve high performance lithium-ion batteries. *Energy Environ. Sci.* 11, 669–681. doi: 10.1039/c8ee00239h
- Zhang, Q., Liu, Z., Zhao, B., Cheng, Y., Zhang, L., Wu, H.-H., et al. (2018b). Design and understanding of dendritic mixed-metal hydroxide nanosheets@N-doped carbon nanotube array electrode for high-performance asymmetric supercapacitors. *Energy Storage Mater.* 16, 632–645. doi: 10.1016/j.ensm.2018.06.026
- Zhao, B. T., Zhang, L., Zhang, Q. B., Chen, D. C., Cheng, Y., Deng, X., et al. (2018). Rational design of nickel hydroxide-based nanocrystals on graphene for ultrafast energy storage. *Adv. Energy Mater.* 8:1702247. doi: 10.1002/aenm.201702247
- Zhao, L., Fan, L.-Z., Zhou, M.-Q., Guan, H., Qiao, S., Antonietti, M., et al. (2010). Nitrogen-containing hydrothermal carbons with superior performance in supercapacitors. *Adv. Mater.* 22, 5202–5206. doi: 10.1002/adma.201002647
- Zheng, Z., Zao, Y., Zhang, Q., Cheng, Y., Chen, H., Zhang, K., et al. (2018). Robust erythrocyte-like Fe₂O₃@carbon with yolk-shell structures as high-performance anode for lithium ion batteries. *Chem. Eng. J.* 347, 563–573. doi: 10.1016/j.cej.2018.04.119
- Zhu, C., Wen, D., Leubner, S., Oschatz, M., Liu, W., Holzschuh, M., et al. (2015). Nickel cobalt oxide hollow nanosponges as advanced electrocatalysts for the oxygen evolution reaction. *Chem. Commun.* 51, 7851–7854. doi: 10.1039/c5cc01558h
- Zhu, S., Li, L., Liu, J., Wang, H., Wang, T., Zhang, Y., et al. (2018). Structural directed growth of ultrathin parallel birnessite on beta-MnO₂ for high-performance asymmetric supercapacitors. *ACS Nano* 12, 1033–1042. doi: 10.1021/acsnano.7b03431

Conflict of Interest Statement: The authors declare that the research was conducted in the absence of any commercial or financial relationships that could be construed as a potential conflict of interest.

Copyright © 2019 Huo, Liu, Yuan, Li, Lan, Liu and Zhang. This is an open-access article distributed under the terms of the Creative Commons Attribution License (CC BY). The use, distribution or reproduction in other forums is permitted, provided the original author(s) and the copyright owner(s) are credited and that the original publication in this journal is cited, in accordance with accepted academic practice. No use, distribution or reproduction is permitted which does not comply with these terms.